Articles

Glass Network Evolution with Bi^{3+}/Ti^{4+} Substitution in Phosphate Glasses Formulated with a Constant Oxygen/Phosphorus Ratio. EXAFS, XANES, and ^{31}P Double Quantum MAS NMR

Lionel Montagne,* Sylvie Daviero, and Gérard Palavit

Laboratoire de Cristallochimie et Physicochimie du Solide, Ecole Nationale Supérieure de Chimie de Lille, BP 108, 59652 Villeneuve d'Ascq Cedex, France

Abdelillah Shaim and Mohamed Et-Tabirou

Laboratoire de Physico-Chimie du Solide, Université Ibn Tofail, Faculté des Sciences, BP 133, 14000 Kenitra, Morocco

Received January 8, 2003. Revised Manuscript Received May 22, 2003

This paper reports a structural study of the effect of TiO_2 substitution for Bi_2O_3 in $xNa_2O-xP_2O_5-yBi_2O_3-zTiO_2$ glasses, which were formulated in order to keep a constant average polymerization of the phosphate network. XANES and EXAFS analyses have indicated that the bismuth coordination sphere is similar to that described in other phosphate glasses [Daviero S.; Montagne L.; Palavit G.; Mairesse G.; Belin S.; Briois V. *J. Phys. Chem. Solids* **2003**, *64* (2), 253], and that the titanium coordination sphere is asymmetric, but remains octahedral whatever the substitution degree. ^{31}P double-quantum filtered MAS NMR shows that the Q^2 fraction increases with the titanium content in the glasses, thus revealing a repolymerization of the phosphate network. The consideration of charges on oxygens (in terms of valence units) leads to the conclusion that titanium octahedra are coordinated to both Q^1 and Q^2 sites. The excess charge on these oxygens is compensated by Na^+ removed from Q^1 sites, which explains the observed repolymerization of the phosphate network. The evolution of glass properties is discussed within the context of this structural model. The increase of glass-transition temperature with titanium substitution for bismuth is due to the repolymerization of the phosphate network. The increase of electrical conductivity with titanium content is attributed to an increase of sodium mobility when it is involved in charge compensation of Ti^{4+} octahedra.

Introduction

Bismuth-III and titanium-IV oxides both have a large influence on phosphate glass structure and properties. Bi_2O_3 increases the phosphate glass durability[1] and enables it to keep high expansion coefficients, contrary to Al_2O_3.[2] Titanium oxide containing phosphate glasses have a large range of technological applications: biomaterials,[3] photonic devices,[4,5] semiconductors,[6] and ionic conductors.[7−9] We report here a description of the network of sodium phosphate glasses that contain both Bi_2O_3 and TiO_2, using a complete set of experimental data: the phosphate network is characterized with ^{31}P double-quantum filtered MAS NMR, and cationic environments are examined by XANES and EXAFS for Ti and Bi, and by MAS NMR for Na. We formulated the glasses to keep a constant polymerization level, i.e., we kept constant the oxygen/phosphorus ratio (O/P) for each glass composition by exchanging $3Ti^{4+}$ for $4Bi^{3+}$. The specific effect of Ti^{4+} and Bi^{3+} on the glass network will therefore be monitored, whereas the modification of the cationic environments will be monitored with X-ray absorption spectroscopy.

Using a complementary multi-spectroscopic approach with ^{31}P MAS NMR, double quantum filtered MAS NMR, FTIR, XANES and EXAFS at Bi L_{III} edge, we

* To whom correspondence should be addressed. Tel: (33) 3 20 43 41 86. Fax: (33) 3 20 33 72 46. E-mail: lionel.montagne@univ-lille1.fr.

(1) Peng, Y. B.; Day, D. E. *Glass Technol.* **1991**, *32* (5), 166.
(2) Montagne, L.; Palavit, G.; Mairesse, G.; Draoui, M.; Aomari, K.; M. Saidi Idrissi *Phys. Chem. Glasses* **1997**, *38* (1), 15.
(3) Hosono, H.; Abe, Y. *J. Non-Cryst. Solids* **1995**, *190*, 185.
(4) Cardinal, T.; Fargin, E.; Nazabal, V.; LeFlem, G.; Le Boiteux, S.; Ducasse, L. *J. Non-Cryst. Solids* **1998**, *239*, 131.
(5) Sigaev, V. N.; Pernice, P.; Aronne, A.; Akimova, O. V.; Stefanovich, S. Y.; Scaglione, A. *J. Non-Cryst. Solids* **2001**, *292*, 59.
(6) Hayashi, T.; Saito, H. *Phys. Chem. Glasses* **1979**, *20* (5), 108.
(7) Kishioka, A.; Rousselot, C.; Malugani, J. P.; Mercier, R. *Phosphorus Res. Bull.* **1991**, *1*, 387.
(8) Sobha, K. C.; Rao, K. J. *J. Non-Cryst. Solids* **1996**, *201*, 52.
(9) Montagne, L.; Palavit, G.; Shaim, A.; Et-Tabirou, M.; Hartmann, P.; Jäger, C. *J. Non-Cryst. Solids* **2001**, *293−295*, 719.

10.1021/cm0310061 CCC: $25.00
Published on Web 11/13/2003

have previously described the effect of introducing Bi^{3+} ions into a sodium phosphate glass network.[10,11] From XANES and EXAFS analyses,[11] we showed that a Bi^{3+} environment in sodium phosphate glasses is similar to that observed in the crystalline reference $Na_3Bi(PO_4)_2$, with two oxygen shells. The first shell contains 5.5 ± 0.5 oxygen atoms and EXAFS data are best fitted with a two sub-shell model. The Bi−O distances in this first asymmetric shell do not change with increasing Bi_2O_3 quantity in the glasses, and only a qualitative evolution of the second oxygen shell is observed. The phosphate glass network is depolymerized by Bi_2O_3, and the ^{31}P MAS NMR indicated that all the O^{2-} anions introduced by the dissociation of Bi_2O_3 in the melt are incorporated as nonbridging oxygens into the phosphate network. This structural description is in accordance with a mixed-network former effect of Bi_2O_3 and with the high polarizability of Bi^{3+}, which enables an asymmetric but constant coordination with oxygens, as well as a progressive deformation of the longer oxygen shells when increasing the Bi_2O_3 content in the glass. This structural model explains the linear evolution of density and glass transition temperature with the quantity of Bi_2O_3 in the glass composition.[11] This behavior is different from that observed for other oxides, e.g. Al_2O_3.[12] Indeed, when the Al_2O_3 content increases in the glass, the coordination of Al^{3+} decreases from 6 to 4 to adjust the local electronic density on $P-O_{nb}$ bonds, leading to a nonlinear evolution of the glass properties.[13]

Many studies have dealt with the structure of titanophosphate glasses, mainly because the empty d-shell of Ti^{4+} ions contributes to the large increase of the linear and nonlinear optical indices of the glasses,[4,14] thus providing promising technological applications. In titanophosphate and calcium titanophosphate glasses, Raman and ^{31}P MAS NMR spectroscopies have shown that for a TiO_2 content ranging from 30 to 70 mol %, distorted 5- and 6-six coordinated Ti polyhedra are linked to orthophosphates through Ti−O−P bonds.[15] It was concluded that the glass network is very similar to NASICON ionic conducting materials.[15] The occurrence of Ti−O−Ti bonds in these high TiO_2 glasses was characterized with Raman spectroscopy[15] and X-ray absorption.[16] In phosphate and borophosphate glasses, EXAFS, XANES,[16] and neutron diffraction[7] studies concluded that the nonlinear refractive indices originate from highly polarizable asymmetric Ti(5) and Ti(6) oxygenated units. The amount of 5-fold Ti is significant only above 15 mol %. We then reported a structural description of the phosphate network of $50Na_2O-xTiO_2-(50-x)P_2O_5$ glasses, in which the TiO_2 concentration is less than 15 mol %, low enough to expect no Ti−O−Ti bonds.[9] ^{31}P MAS NMR indicated that the phosphate network is mainly made of short chains and dimeric units. The connectivity between these phosphate units was characterized by double-quantum filtered ^{31}P MAS NMR, which showed that diphosphate units bonded to both sodium and titanium are present even at the lowest titanium concentration.[9]

There is an interest in combining the effects of Bi_2O_3 and TiO_2 on phosphate glass properties.[17] As was observed for the combined effect of Al_2O_3 and Bi_2O_3 in sodium phosphate glasses[2], we can expect that the high polarizabilities of Bi^{3+} and Ti^{4+} will improve the glass properties. Particularly, it may enhance the Na^+ mobility in the glass matrix.

Table 1. Compositions of the Glasses[a]

Na_2O x	P_2O_5 x	Bi_2O_3 y	TiO_2 z	O/P
45.5 (45.8)	45.9 (45.8)	0 (0)	8.6 (8.5)	3.183 (3.185)
45.9 (46.1)	46.1 (46.1)	1.4 (1.5)	6.5 (6.3)	3.185 (3.185)
46.2 (46.4)	46.4 (46.4)	2.6 (2.8)	4.8 (4.4)	3.185 (3.185)
46.3 (46.7)	46.8 (46.7)	4.2 (4.1)	2.8 (2.5)	3.189 (3.185)
46.8 (47.1)	47.2 (47.1)	6.0 (5.8)	0 (0)	3.186 (3.185)

[a] The values in parentheses are the batch compositions.

Experimental Procedures

The glasses were prepared by melting Bi_2O_3, TiO_2, and $NaPO_3$ in a platinum crucible, between 1000 and 1100 °C, for 2 h with intermediate homogenizations. The melts were quenched on a water-cooled brass plate. The glasses were then analyzed by energy dispersive spectrometry (EDS) (the compositions are reported in Table 1).

The glasses are pale purple, due to the presence of a small amount of Ti^{3+}, as reported by other authors.[15,18] An evaluation of the quantity of Ti^{3+} paramagnetic species was obtained from the magnetization curve measured at 30 K, with an applied field ranging from 0 to 3 T, on 0.1207 g of $45.9Na_2O-46.1P_2O_5-1.4Bi_2O_3-6.5TiO_2$ glass. It was measured with an Oxford Instrument vibrating sample magnetometer with a typical sensitivity of 10^{-8} emu. Considering that

$$m/H = \frac{np^2{\mu_B}^2\mu_0}{(3kT)}$$

where m is the magnetic moment, H is the magnetic field, n is the number of magnetic cations, μ_0 is the permeability of free space, μ_B is the Bohr magneton, k is the Boltzmann constant, and p is the effective moment of the cations

$$p = 2[S(S+1)]^{1/2}$$

and $p = 1.73$ for Ti^{3+} in a spin-only approximation.

Consequently, it is deduced that $n(Ti^{3+}) \leq 2 \times 10^{13}$. As the ratio of Ti^{3+}:Ti_{total} is less than 4×10^{-5}, the low content of Ti^{3+} ions in the measured glass can be neglected. We assume that the Ti^{3+} content is also negligible in all the glasses studied here.

The one-dimensional ^{31}P MAS NMR spectra were recorded on a Bruker ASX100 spectrometer operating at 2.34 T, with a 1.5 μs pulse (45°), and a 60 s delay between each accumulation, to enable sufficient relaxation. A 7-mm MAS probe was used. The ^{31}P double quantum spectra were also recorded at 2.34 T. The spinning frequency was 5 kHz, which leads to time increments of 200 μs for recording the two-dimensional rotor synchronized spectra. The back-to-back[19,20] acquisition sequence was used. A total of 16 pulses of 3.5 μs (90°) were used

(10) Montagne, L.; Palavit, G.; Mairesse, G. *Phys. Chem. Glasses* **1996**, *37* (5), 206.
(11) Daviero, S.; Montagne, L.; Palavit, G.; Mairesse, G.; Belin, S.; Briois, V. *J. Phys. Chem. Solids* **2003**, *64* (2), 253.
(12) Brow, R. K. *J. Am. Ceram. Soc.* **1993**, *76* (4), 913.
(13) Brow, R. K. *J. Am. Ceram. Soc.* **1993**, *76* (4), 919.
(14) Vogel, E. M.; Weber, M. J.; Krol, D. M. *Phys. Chem. Glasses* **1991**, *32* (6), 231.
(15) Brow, K.; Tallant, D. R.; Warren, W. L.; McIntyre, A.; Day, D. E. *Phys. Chem. Glasses* **1997**, *38* (6), 300.
(16) Cardinal, T.; Fargin, E.; Le Luyer, Y.; Le Flem, G.; Canioni, L.; Segonds, P.; Sarger, L.; Adamietz, F.; Ducasse, A. *Nucl. Instr. Methods* **1995**, *B97*, 169.
(17) Shaim, A.; Et-tabirou, M.; Montagne, L.; Palavit, G. *Mater. Res. Bull.* **2002**, *37* (15), 2459.
(18) Bausa, L. E.; Jaque, F.; Garcia Sole, J.; Cases, R.; Duran, A. *J. Luminescense* **1988**, *40−41*, 193.
(19) Feike, M.; Graf, R.; Schnell, I.; Jäger, C.; Speiss, H. W. *J. Am. Chem. Soc.* **1996**, *1189*, 631.

for both the excitation and reconversion of double quantum coherences, thus giving a total excitation/reconversion time of 400 μs. The repetition time was 10 s (presaturation was used, and 0.1 w% paramagnetic Co_3O_4 was added to the glasses to decrease the relaxation time) and 16 accumulations were used. A total of 256 increments was necessary in the t_1 dimension to record the whole signal. The DQ spectra are shown as contour plots. The ^{31}P NMR chemical shifts are referenced to an 85% H_3PO_4 solution at 0 ppm. The $Q^{n,ij}{}_{(M)}$ notation, introduced by Witter et al.,[21] is used in this paper: n is the number of bridging oxygens bonded to a given PO_4 site, i and j indicate the nature of the other Q^n sites bonded through these bridging oxygens, and (M) indicates which cation is charge compensating for this PO_4 site. The MAS NMR spectra were fitted with the DM-FIT software.[22] Gaussian lines were used because the ^{31}P resonances in glasses are dominated by chemical shift distribution. A small Lorentzian contribution (ca. 5%) was, however, introduced to optimize the fit.

The ^{23}Na NMR spectra were recorded at 9.4 T on a Bruker AV-400 spectrometer (Larmor frequency 105.8 MHz). The MAS spinning rate was 15 kHz, the pulse length was 2 μs, and the repetition rate was 5 s. The chemical shift reference for ^{23}Na was a 1 M NaCl solution.

For the XANES and EXAFS analyses, the samples, finely powdered and thoroughly mixed with cellulose, were pressed into pellets and sandwiched between two Kapton adhesive tapes. The quantities were chosen to have at the absorption edge a jump close to one for the X-ray absorption coefficient. X-ray absorption spectra were collected at the titanium K-edge (4966 eV) and the Bi L_{III} edge (13 426 keV), using synchrotron radiation at LURE, Orsay, on EXAFS 4, in the D44 beamline from DCI. All The EXAFS and XANES data were collected at liquid nitrogen temperature (77 K) in transmission mode, using a Si (111) double crystal monochromator for the EXAFS spectra, and Si (311) for the XANES spectra. The titanium XANES and EXAFS spectra were recorded with 0.2 and 2 eV steps, respectively, with 2 s accumulation at each step. For the bismuth spectra, the steps were 0.5 and 4 eV respectively. The absorption coefficients were determined by recording the flux intensity before (I_o) and after (I_1) the sample, using two ionization chambers filled with nitrogen and argon mixture. Titanium and bismuth XANES spectral analyses were normalized with a victoreen function to fit the region before the preedge and subtracting this as background absorption. Then, the spectra were normalized by using the beginning of EXAFS oscillations as a reference unit. The energy calibration of the monochromator was checked between the spectra using a Ti and Pb metal foil. EXAFS data analyses were carried out using the standard method.[23,24] After absorption background subtraction, and a fit by a victoreen function from the rough data before the edge, the EXAFS signal was calculated using the Lengeler−Eisenberger method[25] and converted into a function of the wave vector $k\chi(k)$. The data were Fourier transformed using k^3 ponderation and a Kaiser window with $\tau = 2.5$, leading to a distance scale spectrum in nm. The peak corresponding to the first oxygen shell around the metal was then filtered and back-transformed to k-space. The resulting EXAFS signal can be expressed by

$$k\chi(k) = S_0{}^2 \sum_i \frac{Ni}{R_i{}^2} e^{-2k^2\sigma_i{}^2} e^{-2R_i\Gamma/\kappa} f_{ij}(\pi,k) \sin [2kR_i + \Phi_i(k)] \quad (1)$$

where Ni is the number of atoms in the coordination shell i at the average atomic distance Ri from the absorbing atom; $\sigma(i)$ is the Debye−Waller factor, $\lambda(k)$is the electron mean-free-path, $S_o{}^2$ is an amplitude reduction factor due to many-body effects,

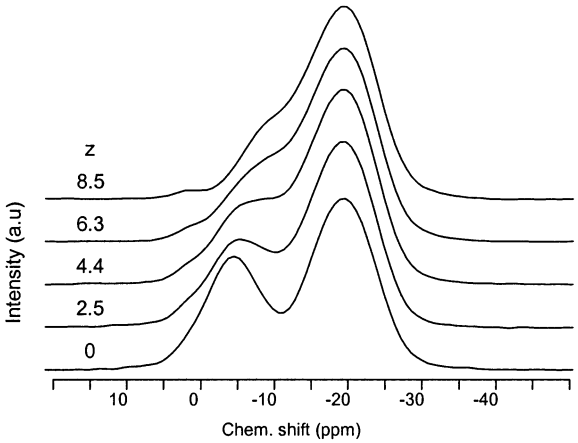

Figure 1. ^{31}P MAS NMR (DQ MAS NMR) spectra of xNa$_2$O−xP$_2$O$_5$−yBi$_2$O$_3$−zTiO$_2$ glasses. See Table 1 for the glass compositions.

and $f_{ij}(\pi,k)$ and $\Phi_i(k)$ are the amplitude and phase function of the coordination shell, respectively, which are obtained from the McKale tabulated functions.[26,27] These functions have been tested on crystalline references TiO_2 and $Na_3Bi(PO_4)_2$, to determine the threshold energy ($E_0 + \Delta E$) and the electron mean free path (Γ) through the relation $\lambda(k) = k/\Gamma$. The Fourier-filtered signals obtained for the glasses were simulated by a least-squares refinement, leading to the determination of the structural parameters R, N, and σ for the first coordination shell. The reliability of the fit is given by the value of the residual function ρ defined as follows:

$$\rho = \sum_i k_i[\chi_{\text{exp}}(k_i) - \chi_{th}(k_i)]^2 / \sum_i k\chi_{\text{exp}}(k_i)^2 \quad (2)$$

TiO_2 anatase and 26K$_2$O−27TiO$_2$−47SiO$_2$ glass (KTS) were used as references for 6-fold and 5-fold Ti coordination, respectively. For sensitivity reasons, EXAFS and XANES spectra were recorded on the glasses with high Ti and Bi contents.

The glass transition temperatures were measured with a differential scanning calorimeter at a heating rate of 5 K·mn^{-1}. For the electrical measurements, gold electrodes were vacuum deposited on both sides of the polished samples. The conductivities were obtained by complex impedance spectroscopy in a $1-10^6$ Hz frequency range, using a SOLARTRON 1255 apparatus. The temperature ranged from 30 to 300 °C, with 20 °C steps and a half hour stabilization delay at each temperature increment.

Results

Table 1 reports batch and measured glass compositions. Some differences with the target compositions are observed due to unavoidable losses during preparation. However, the glass compositions remain close enough to the objectives to consider constant the O/P values. Hence, in the following text, the compositions will always refer to the batch compositions.

Figure 1 shows the ^{31}P MAS NMR spectra of xNa$_2$O−xP$_2$O$_5$−yBi$_2$O$_3$−zTiO$_2$ glasses. The spectrum of the z =

(20) Olsen, K. K.; Zwanziger, J. W.; Hartmann, P.; Jäger, C. *J. Non-Cryst. Solids* **1997**, *222*, 199.
(21) Witter, R.; Hartmann, P.; Vogel, J.; Jäger, C. *Solid State Nucl. Magn. Reson.* **1998**, *13* (3), 189.
(22) Massiot, D.; Fayon, F.; Capron, M.; King, I.; Le Calvé, S.; Alonso, B.; Durand, J.−O.; Bujoli, B.; Gan, Z.; Hoatson, G. *Magn. Reson. Chem.* **2002**, *40*, 70.
(23) Konigsberger, D. C.; Prins Chemical, R. In *Analysis*; Vol. 92, X-Ray Absorption: Principles, Applications, Techniques of EXAFS, SEXAFS, and XANES; J. Wiley & Sons: New York, 1988.
(24) Michalowicz, A. In *EXAFS pour le Mac;* Société Française de Chimie: Paris, 1991; p 102.
(25) Lengeler, B.; Eisenberger, P. *Phys. Rev.* **1980**, *B 21*, 4507.
(26) McKale, A. G.; Veal, B. W.; Paulikas, A. P.; Chan, S. K.; Knapp, G. S. *J. Am. Chem. Soc.* **1988**, *110*, 3763.
(27) McKale, A. G.; Veal, B. W.; Paulikas, A. P.; Chan, S. K.; Knapp, G. S.; *Physica B* **1989**, *158* (1−3), 355.

0 glass shows two broad resonances at −4 and −19.5 ppm. According to previous results,[10] they are attributed to Q^1 and Q^2 sites, respectively. These chemical shift values indicate that the nonbridging oxygens of the Q^2 sites are ionically bonded to Na^+ (same chemical shift as sodium metaphosphate glass $NaPO_3$[28]), and that the Q^1 sites are bonded to Bi^{3+} (high field shift compared to Q^1 in $Na_2O-P_2O_5$ glasses[10]). Substitution of TiO_2 for Bi_2O_3 does not change the chemical shift of the Q^2 resonance (Figure 1), but a shift to high field of the Q^1 resonance is observed, due to the influence of Ti^{4+}. A small but significant resonance is observed on the low field side (+2 ppm) of the MAS NMR spectra of $z \geq 2.5$ glasses (Figure 1), although its presence cannot be excluded on the $z = 0$ glass spectrum. It is attributed to Q^0 sites (monophosphate groups), connected to both Na^+ and Ti^{4+} and/or Bi^{3+} ($Q^0_{Na,Ti,Bi}$), because the chemical shift of Q^0_{Na} is +13 ppm[29] and the bonding to Ti^{4+} or Bi^{3+} results in a high field shift of Q^n sites.[9,10]

A more accurate description of the phosphate network can be obtained with double-quantum filtered ^{31}P MAS NMR. This recently introduced method[30] enables evaluation of the spatial proximity of Q^n sites. During the evolution of magnetization under double quantum coherence, the dipolar interactions removed under MAS conditions are reintroduced. 'Because the dipolar interactions are proportional to r^{-3} (r is the internuclear distance), the double quantum filtered signals contain information about distance. On the two-dimensional double quantum spectra, signals lying on the diagonal are self-correlated, whereas off-diagonal signals indicate connectivity between different Q^n units. For instance, Q^1 sites of pyrophosphates (diphosphates) are located on the diagonal, whereas Q^1 sites of chain-end groups, which are correlated to Q^2, are located off-diagonal. Thus, this method provides a powerful tool for characterizing the polymerization of the phosphate glass network.[21] On double quantum spectra, the horizontal axis is equivalent to the MAS spectrum (F2 dimension), and the vertical axis is the isotropic dimension (F1), the projection of which gives a double quantum filtered spectrum. The resonances are located by their (F2, F1) coordinates. Figure 2 shows the double quantum filtered ^{31}P MAS NMR (DQ MAS NMR) spectra of 3 glasses. A total of 4 resonances are seen on the spectrum of the $z = 0$ glass. The main resonance is located at (−19.5, −39) ppm. According to its position on the diagonal and its F2 chemical shift, it is assigned to Q^2 sites connected to similar Q^2 sites, i.e., Q^2 sites located in metaphosphate chains. According to the notation introduced by Witter et al.,[21] they are called $Q^{2,22}$. The second resonance located on the diagonal at (−3, −6) ppm is ascribed to self-correlated Q^1 sites, meaning diphosphate groups ($Q^{1,1}$). The two off-diagonal resonances at (−4, −24) ppm and (−19, −24) ppm are assigned to $Q^{1,2}$ sites that are connected to $Q^{2,12}$ sites, i.e., to chain-end groups. When Ti^{4+} is substituted for Bi^{3+}, the 1D MAS NMR spectra are less resolved because of the increased overlapping of the Q^2 and Q^1 sites. However, DQ MAS NMR spectra (Figure 2) show that the connectivities are qualitatively preserved, with the presence of diphosphate as well as chain-end groups in the glasses containing titanium. In accordance with what is expected for isolated Q^0 sites, Q^0 sites are not detected on DQ spectra. However, their low content may prevent their detection after the double quantum filter.

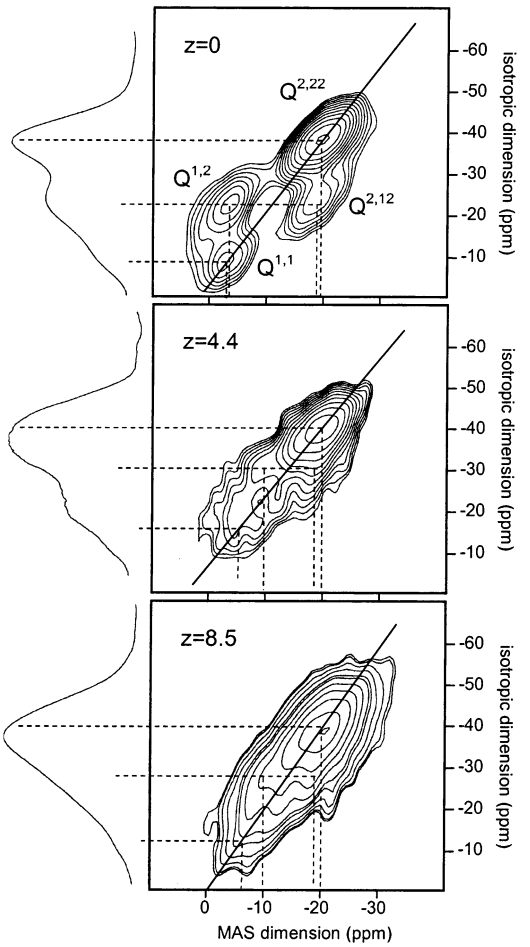

Figure 2. Double quantum filtered ^{31}P MAS NMR (DQ MAS NMR) spectra of $xNa_2O-xP_2O_5-yBi_2O_3-zTiO_2$ glasses. The isotropic projections are shown on the left side of the spectrum. See Table 1 for the glass compositions. Dotted lines indicate the position of the Q^n resonances mentioned in the text.

Quantification of the Q^n sites cannot be obtained directly from ^{31}P DQ MAS NMR spectra because double quantum coherences are not systematically quantitatively excited and detected.[21] The sites identified on DQ spectra are then quantified on 1D MAS NMR spectra, their chemical shift being used as a constraint for the spectral decomposition (Figure 3). A difficulty arises because the chemical shifts of diphosphate ($Q^{1,1}$) and of chain-end groups ($Q^{1,2}$) are not sufficiently different to allow for a distinct contribution in the 1D spectra decomposition of the glass $z = 0$ (Figure 2). Moreover, the Q^2 sites ($Q^{2,22}$ and $Q^{2,12}$) are not always resolved on the spectra of all the glasses. Fortunately, DQ NMR spectra indicate that Q^1 and Q^2 sites have distinct contributions on the MAS NMR spectra, even for the least resolved spectrum ($z = 8.5$). The spectra were thus decomposed into Q^1 sites (including $Q^{1,1}$ and $Q^{1,2}$ for the $z = 0$ glass spectrum) and Q^2 sites (including $Q^{2,1}$ and $Q^{2,2}$). Figure 4 shows that the chemical shift of Q^0 and Q^2 sites does not change with the Ti^{4+}/Bi^{3+} substitution,

(28) Brow, R. K.; Phifer, C. C.; Turner, G. L.; Kirkpatrick, R. J. *J. Am. Ceram. Soc.* **1991**, *74* (6), 1287.

(29) Duncan, T. M. In *A Compilation of Chemical Shift Anisotropies*; Farragut Press: Chicago, IL, 1990; p 12.

(30) Jäger, C.; Hartmann, P.; Witter, R.; Braun, M. *J. Non-Cryst. Solids* **2000**, *263&264*, 61.

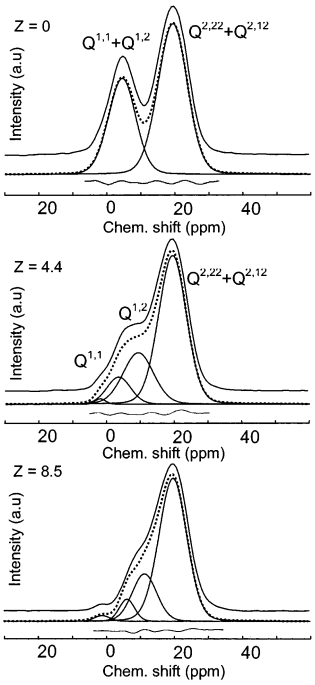

Figure 3. Decomposition of ^{31}P MAS NMR spectra of $xNa_2O-xP_2O_5-yBi_2O_3-zTiO_2$ glasses. The continuous line is the experimental spectrum, and the dotted line is the simulated spectrum. The difference spectrum-fit is shown below.

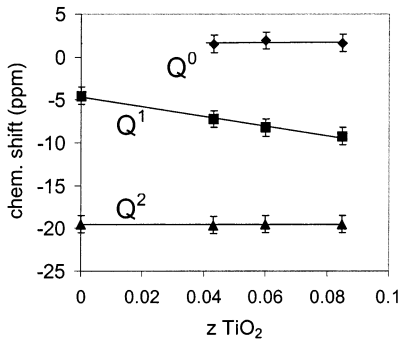

Figure 4. Chemical shift of Q^n sites (obtained from the decomposition of ^{31}P MAS NMR spectra) versus the TiO_2 content in $xNa_2O-xP_2O_5-yBi_2O_3-zTiO_2$ glasses.

whereas Q^1 sites are shifted to high field. This means that Bi and Ti bonding to the phosphate network occur mainly via Q^1 sites and not via Q^2 sites. Q^2 sites remain bonded to sodium ions. The nonevolution of Q^0 chemical shift may indicate a preferential bonding to titanium or bismuth ions, but their low content does not enable a definite conclusion. Figure 5 reveals a modification of the relative amount of Q^1 and Q^2 sites with the substitution of Ti^{4+} for Bi^{3+}. The relative proportion of Q^2 sites increases from 60 to 77%, and the proportion of Q^1 decreases from 40 to 21%. There is also a small increase in the content of Q^0 sites. This evolution of the relative amount of Q^n sites is in contradiction with the constant oxygen/phosphorus (O/P) ratio of the glasses (taking into account the variations due to measurement incertitudes). This point will be discussed later.

^{23}Na MAS NMR spectra (not shown here) exhibit a broad and asymmetric resonance typical of chemical shift and quadrupolar constant distribution in glasses.[31] A shift to high field occurs as TiO_2 is introduced in the compositions, which means that although ^{31}P NMR

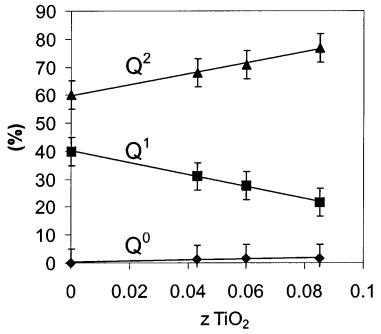

Figure 5. Relative number of Q^n sites (obtained from the decomposition of ^{31}P MAS NMR spectra) versus the TiO_2 content in $xNa_2O-xP_2O_5-yBi_2O_3-zTiO_{22}$ glasses.

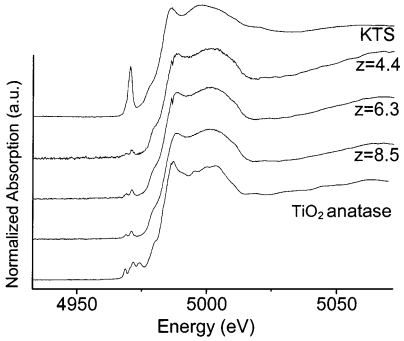

Figure 6. XANES spectra at Ti−K edge of $xNa_2O-xP_2O_5-yBi_2O_3-zTiO_2$ glasses, TiO_2 anatase, and $26K_2O-27TiO_2-47SiO_2$ glass (KTS).

indicates that sodium ions are mainly bonded to Q^2 sites, they also contribute to the charge compensation of Q^1 and Q^0 sites.[28] They may also be involved in the charge compensation of units, different from the phosphate network, as will be discussed below.

Farges et al.[32−34] have shown that accurate information on the titanium environment can be extracted from XANES spectra by comparing the energy and height of the preedge peak. Ti K-edge XANES spectra of phosphate glasses, TiO_2 (6-fold Ti coordination), and $26K_2O-27TiO_2-47SiO_2$ glass (5-fold Ti coordination) are presented in Figure 6. A closer inspection of the preedge energies and heights, Figure 7, indicates a major amount of octahedral Ti. The shift at lower energies (4972 eV) of the main pre-peak suggests the presence of only a small amount of five-coordinated Ti. This feature is common for all the studied glasses.

The Fourier transformed spectra of the normalized *k* weighted EXAFS spectra, with uncorrected phase shift and amplitude, are shown in Figure 8. The large peak near 1.9 Å corresponds to backscattering from the first neighbor-oxygen atoms. The smaller peaks, appearing at larger distances, are due to the backscattering of Na, P, and perhaps Bi atoms. The first oxygen shell was fitted with two distances to take into account the site asymmetry. The fitting results are reported in Table 2

(31) Mackenzie, K. J. D.; Smith, M. E. in *Multinuclear Solid-State NMR of Inorganic Materials*; Pergamon Materials Series vol. 6,;. Pergamon: London, 2002; p 415.
(32) Farges, F.; Brown, G. E.; Rehr, J. *Geochim. Cosmochim. Acta* **1996**, *60* (16), 3023.
(33) Farges, F.; Brown, G. E.; Rehr, J. *Geochim. Cosmochim. Acta* **1996**, *60* (16), 3039.
(34) Farges, F.; Brown, G. E.; Rehr, J. *Phys. Rev. B* **1997**, *56* (4), 1809.

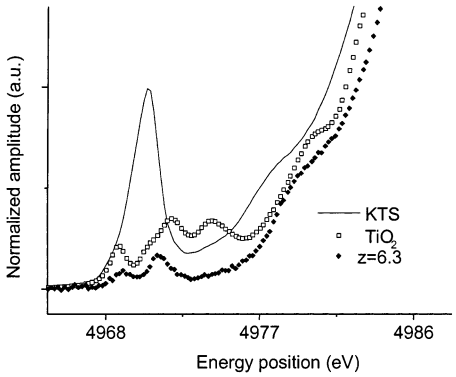

Figure 7. Titanium XANES pre-peak structures of TiO_2 (six coordinated Ti), KTS glass (five coordinated Ti), and $46.1Na_2O-46.1P_2O_5-1.5Bi_2O_3-6.3TiO_2$ glass.

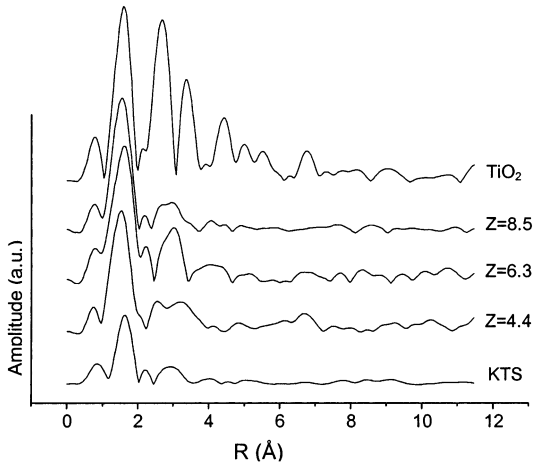

Figure 8. Fourier transform of Ti EXAFS spectra, with uncorrected phase shift and amplitude, of $xNa_2O-xP_2O_5-yBi_2O_3-zTiO_2$ glasses, KTS glass, and TiO_2 anatase.

Table 2. Fitting Results of Titanium K-Edge EXAFS Spectra[a]

$zTiO_2$	4.4	6.5	8.5	KTS
N_1	2.80	2.33	4.02	1.29
N_2	3.20	3.66	2.03	3.68
R_1 (Å)	1.91	1.87	1.94	1.72
R_2 (Å)	2.05	2.01	2.03	1.98
Γ	0.993	0.993	0.993	0.993
σ_1	0.02	0.01	0.07	0.10
σ_2	0.04	0.01	0.07	0.07
ΔE_1 (eV)	5.13	3.93	5.11	12.46
ΔE_2 (eV)	7.38	3.20	4.90	5.49
ρ	6.3×10^{-3}	1.0×10^{-2}	4.7×10^{-3}	7.0×10^{-3}

[a] N, coordination number; R, bond length; Γ, electron mean free path; σ, Debye−Waller factor; ΔE, threshold energy; ρ, reliability of the fit (see text).

and some fitted spectra are presented in Figure 9. The EXAFS data confirm the XANES observations: titanium coordination sphere is octahedral in all characterized glasses. Moreover, this coordination sphere is asymmetric, which suggests a bonding with different phosphate units, as will be discussed later.

The comparison of XANES spectra at BiL_{III} (not shown here) reveals a Bi local environment close to that of $Na_3Bi(PO_4)_2$, thus justifying the use of this crystalline compound as a reference for the EXAFS simulations.[11] In $Na_3Bi(PO_4)_2$, 8 oxygen atoms surround the bismuth cation.[35] The presence of the $6s^2$ electronic lone pair highly distorts this environment. By consequence, three

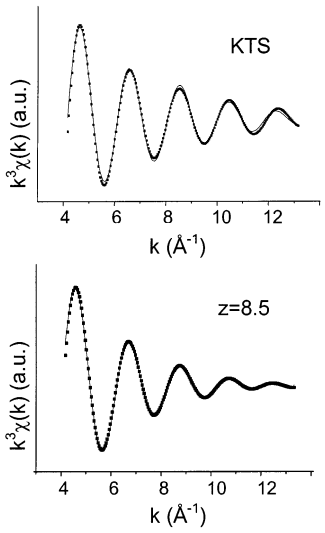

Figure 9. Ti K-edge EXAFS functions generated by back-transforming the first peak of radial function (first coordination shell) for the KTS glass and $45.8Na_2O-45.8P_2O_5-8.5TiO_2$ glass (dotted line, experimental; continuous line, least-squares fit).

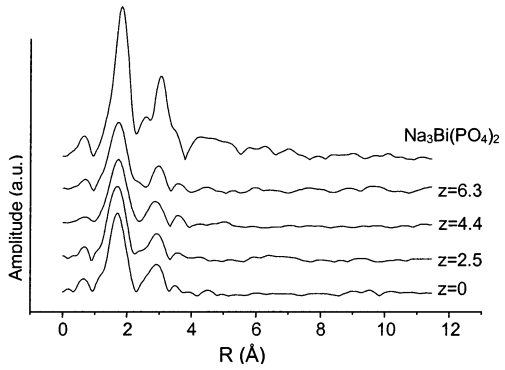

Figure 10. Fourier transform of Bi EXAFS spectra, with uncorrected phase shift and amplitude, of $xNa_2O-xP_2O_5-yBi_2O_3-zTiO_2$ glasses, and $Na_3Bi(PO_4)_2$.

different shells involving O, P, and Na atoms must be considered: a first shell of 5 oxygen atoms at an average distance of 2.35 Å, but ranging between 2.25 and 2.45 Å, a second shell containing 3 longer Bi−O distances between 2.80 and 2.90 Å, and a third one composed of sodium, phosphorus, and maybe titanium atoms at distances above 3.13 Å. Figure 10 shows the Bi L_{III} $k\chi$-(k) EXAFS spectra Fourier Transform |F(r)| with uncorrected phase shift and amplitude, for the different glasses and the $Na_3Bi(PO_4)_2$ reference. In accordance with the above description of the crystal structure,[35] three peaks are observed. The first one near 1.9 Å is attributed to the short Bi−O distances. The data were fitted with a two sub-shell model, close to the reference structure of $Na_3Bi(PO_4)_2$,[11] with 3 oxygen atoms at 2.26 Å and 2 oxygen atoms at 2.40 Å. The obtained structural parameters are reported in Table 3. These results lead to the conclusion that the bismuth environment is very similar to that observed in other phosphate glasses,[11] and that it remains constant upon substitution with titanium.

(35) Mairesse, G.; Drache, M.; Nowogrocki, G.; Abraham, F. *Phase Transitions* **1990**, *27*, 91.

Table 3. Fitting Results of Bismuth L_{III}-edge EXAFS Spectra (Same Symbols as in Table 2)

$zTiO_2$	0	2.5	4.4	6.3
N_1	2.93	2.53	3.18	2.82
N_2	2.07	3.56	1.81	2.19
R_1 (Å)	2.25	2.23	2.25	2.23
R_2 (Å)	2.39	2.35	2.40	2.36
Γ	0.888	0.888	0.888	0.888
σ_1	0.09	0.09	0.09	0.09
σ_2	0.105	0.11	0.10	0.11
ΔE_1 (eV)	5.47	5.85	5.97	6.35
ΔE_2 (eV)	−2.69	−2.79	−2.52	−2.77
ρ	8.2×10^{-3}	7.5×10^{-3}	7.5×10^{-3}	7.0×10^{-3}

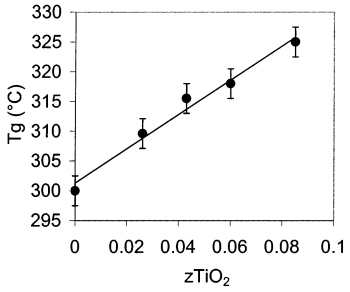

Figure 11. Temperature of glass transition of $xNa_2O-xP_2O_5-yBi_2O_3-zTiO_2$ glasses versus z.

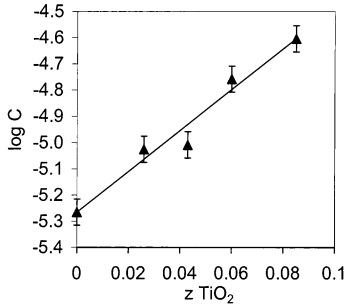

Figure 12. Log$C$ versus z of $xNa_2O-xP_2O_5-yBi_2O_3-zTiO_2$ glasses. The conductivity, C, is expressed in $\Omega^{-1}\cdot cm^{-1}$, and measured at 200 °C.

Figure 11 reports the temperature of glass transition of $xNa_2O-xP_2O_5-yBi_2O_3-zTiO_2$ glasses. It increases linearly with the TiO_2 content in the glass. Considering the substitution of Ti^{4+} for Bi^{3+} is conducted at constant O/P ratio, it means that the atomic content decreases (3Ti for 4Bi). Hence, we conclude that the constant increase in Tg is mainly due to an increase of the network polymerization, and not to a change in the iono-covalency of P−O−Ti bonds compared to P−O−Bi. The increase in Tg can be related to the constant decrease of Q^1 and increase of Q^2 sites (Figure 5).

Figure 12 shows that the glass conductivity increases with the TiO_2 content. The ionic conductivity, C, can be expressed as[36]

$$C = N\mu e^{-Ea/kT}$$

where N is the number of charge carriers and μ is their electrical mobility; $e^{-Ea/kT}$ is the Arrhenius term of the temperature dependence. The electrical conductivity is due to Na^+ transport in such a glass matrix.[36] Because the quantity of Na^+ decreases with the substitution of Ti^{4+} for Bi^{3+} (Table 1), we conclude that the increase in conductivity is due to an increased mobility of Na^+ ions in the glass matrix. This point will be discussed in relation with the structural results below.

Discussion

As mentioned in the Introduction, glass formulations were chosen in order to keep constant the O/P ratio (substitution of $3Ti^{4+}$ for $4Bi^{3+}$). According to previous studies on phosphate glasses,[13,37] this constant O/P ratio means that the polymerization of the phosphate network should remain constant, provided that all oxygen atoms are bonded to PO_4 groups (thus assuming no Bi−O−Bi, Ti−O−Ti, or Ti═O bonds). The ^{31}P MAS NMR spectrum of the glass with only Bi_2O_3 ($z = 0$) shows two well-separated Q^1 and Q^2 resonances (Figure 1). The decomposition of the spectra indicates that the fraction of Q^2 sites (Figure 5), is 0.6(0), which is in good accordance with the measured composition (Table 1) of 0.6(3). This confirms that the Bi_2O_3 dissociation in the glass is complete, according to the schematic reactions

$$Bi_2O_3 = 2Bi^{3+} + 3O^{2-}$$

$$P-O-P + O^{2-} = 2PO^-$$

$$Bi_2O_3 + 3P-O-P = 2Bi(OP)_3$$

XANES and EXAFS data indicate that the bismuth environment, although asymmetric, remains unchanged in all analyzed glasses. Thus, we can assume that the above reactions are valid for all the studied glasses, and that the bismuth does not play a significant role in the network evolution with titanium substitution.

EXAFS and XANES data are also in accordance with a constant coordination sphere of titanium in the glasses studied in this paper. Its coordination sphere always contains 6 oxygen atoms located on a distorted octahedron. A significant amount of lower titanium coordinations, like TiO_5 units, were reported by Brow[15] and Fargin[38] in phosphate glasses, but only for higher titanium concentrations (up to 30 mol %).

Although the glass containing only Bi_2O_3 exhibits the expected Q^2 fraction, double quantum filtered ^{31}P MAS NMR revealed that the substitution of TiO_2 for Bi_2O_3 modified the polymerization of the phosphate network. Indeed, Figure 5 shows that the amount of Q^2 units increases at the expense of Q^1 units, thus indicating a repolymerization of the network. This may be due to some redistribution of oxygens atoms in Ti−O−Ti bonds, i.e., oxygens not involved in P−O−P bonds. However, such Ti−O−Ti bonds are not expected in our glasses because they were not characterized by neutron diffraction in $NaPO_3-TiO_2$ pseudo-binary glasses, even for the highest TiO_2 concentration.[7] The bond valence model can be used to explain the increase of Q^2 sites with the substitution of TiO_2 for Bi_2O_3: if the titanium coordination sphere was a symmetric octahedron, each Ti−O bond would support $^1/_6$ of the Ti^{4+} charge, meaning

(36) Desportes, C.; Duclot, M.; Fabry, P.; Fouletier, J.; Hammou, A.; Kleitz, M.; Siebert, E.; Souquet, J. L. In *Electrochimie des Solides*; PUG: Grenoble, France, 1994; p 130.

(37) Hussein, R.; Holland, D.; Dupree, R. *J. Non-Cryst. Solids* **2002**, *298*, 32.

(38) Fargin, E.; Duchesne, C.; Olazcuaga, R.; LeFlem, G.; Cartier, C.; Canioni, L.; Segonds, P.; Sarger, L.; Ducasse, A. *J. Non-Cryst. Solids* **1994**, *168*, 132.

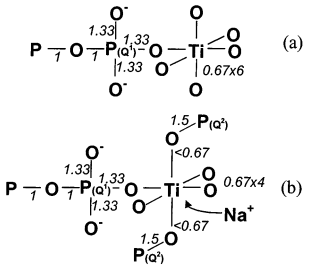

Figure 13. Valence unit models for the bonding of (a) symmetric and (b) asymmetric octahedral Ti^{4+} bonded to phosphate groups.

0.67 vu (valence unit) (Figure 13). This would be an efficient charge compensation for the bonding with $6Q^1$ sites, because each $P_{(Q1)}-O^-$ brings 1.33 vu. Now, if we consider the asymmetric coordination sphere deduced from EXAFS data, a longer Ti−O bond length suggests that its supported charge is less than 0.67 vu (Figure 13). Their bonding is then more probable with Q^2 groups that bring 1.5 vu. However, the Ti−O bond charge cannot decrease to 0.5 v.u., which would result in longer Ti−O bond length. Furthermore, the Q^2 chemical shift did not reveal any bonding with Ti^{4+}. The excess of negative charge that results then on Ti^{4+} can be compensated by Na^+ ions (Figure 13), in the same way as the charge compensation of tetrahedral aluminum in aluminosilicate glasses. The scavenging of some Na^+ ions for the charge compensation of Ti results then in an increase of Q^2 units and a decrease of Q^1 ones, as shown in Figure 5. We notice that the charge compensation of TiO_6 units by sodium ions has no visible effect on the ^{23}Na NMR spectra. This is probably because the number of Na^+ ions involved is much lower than that bonded to nonbridging oxygens.

The presence of P−O−Ti (Q^1(Ti)) resonance overlapping with Q^2 (Na) may explain why the Q^1 relative content decreases (see Figure 5) and thus, would explain why the network polymerization appears to increase. However, the Ti^{4+} contribution is located in the Q^1 resonances ($Q,^{11}$ and Q^{12}) between −5 and −10 ppm. Q^1 sites should be shielded by an averaged contribution of all cations (Na^+, Bi^{3+}, and Ti^{4+}). Hence, the shift to high field with increasing amount of Ti^{4+} (Figures 1, 3, and 4) confirms the effect of Ti^{4+} on these Q^1 sites. Furthermore, there is only one Q^1(Bi, Na) resonance in the $x = 0$ glass, and no contribution overlapping with Q^2, as the calculated network polymerization is in accordance with the O/P ratio. Thus, we do not expect a specific Q^1 resonance at −20 ppm (overlapping with Q^2) for Ti^{4+} if we account only for an averaged bonding. The presence of two kinds of Q^1 resonances on DQ spectra (Q^{11} and Q^{12}) is not contradictory with an averaged bonding, as the correlation of the latter with Q^2 sites (Figure 2) indicates that Q^1 resonances are chain-end groups. The autocorrelation of the former indicates that they are diphosphate units.

Concerning the consequences on the glass properties, we observed that the degree of network polymerization increases. This explains the observed increase of the glass transition temperature (Figure 12). The ionic mobility of sodium ions involved in charge compensation of titanium units is higher than that of sodium ions bonded to nonbridging oxygens, as observed for aluminosilicate glasses.[39] This may contribute to the increased ionic conductivity when TiO_2 is substituted for Bi_2O_3 at constant sodium concentration. However, the amount of Na^+ ions involved in the charge compensation is much lower than those bonded to nonbridging oxygens, hence the increase in ionic conductivity is more probably related to a global change in the network charge. This consequence on ionic mobility will be further reported in another paper.

Conclusion

The effect of TiO_2 substitution for Bi_2O_3 on $xNa_2O-xP_2O_5-yBi_2O_3-zTiO_2$ glass structure and properties was reported. The substitution was formulated in order to keep constant the oxygen/phosphorus ratio, i.e., to keep constant the averaged network polymerization. EXAFS indicates that titanium coordination remains octahedral in each glass, and that its coordination sphere is asymmetric. The increase of Q^2 fraction with titanium substitution is explained with a simple valence unit model: Ti^{4+} are bonded to both Q^1 and Q^2 units, and the excess charge is compensated by Na^+ ions that were removed from Q^1 sites. This glass network model is in accordance with the evolution of glass properties with the substitution of TiO_2 for Bi_2O_3.

Acknowledgment. We thank B. Revel (Centre Commun de Mesure RMN de l'USTL) who recorded the 1D and 2D NMR spectra, and O. Mentré (LCPS) for measuring the Ti^{3+} content. S. Belin and V. Briois (LURE-Orsay) are acknowledged for their help in collecting the XANES and EXAFS data.

CM0310061

(39) Feltz, A. In Glass Science and Technology; Uhlmann, D. R., Kreidl, N. J., Ed.; Academic Press: New York, 1990; Vol. 4 A, p 138.